Available online at www.sciencedirect.com
ScienceDirect
Journal of the European Ceramic Society 27 (2007) 3551–3560
www.elsevier.com/locate/jeurceramsoc

Young's modulus, thermal expansion coefficient and fracture behavior of selected Si–B–C based carbides in the 20–1200 °C temperature range as derived from the behavior of carbon fiber reinforced microcomposites

A. Michaux, C. Sauder, G. Camus *, R. Pailler

Université Bordeaux 1, UMR 5801 (CNRS-SAFRAN-CEA-UB1), Laboratoire des Composites Thermostructuraux, 3 Allée de La Boétie, F-33600 Pessac, France

Received 16 February 2006; received in revised form 4 December 2006; accepted 16 December 2006
Available online 6 April 2007

Abstract

The Young's modulus, thermal expansion coefficient and fracture behavior of different ceramic phases in the Si–B–C system have been determined from room temperature up to 1200 °C using results of tests performed on matrix-dominated carbon fiber reinforced microcomposites by means of a specific high temperature testing apparatus. Results have shown that the boron-rich materials had higher stresses to failure and thermal expansion coefficients than silicon-rich materials whereas all the boron containing materials exhibited a viscoplastic time-dependant mechanical behavior over 1000 °C. The thermoelastic values of the Si–B–C based carbides thus obtained have been used to compute thermal residual stresses in model composite systems, in view of understanding some results reported in the literature regarding the implantation of layered matrices in ceramic matrix composites.

Keywords: Carbides; Mechanical properties; Thermal expansion; Failure analysis; Carbon fibre

1. Introduction

A new concept of self-healing and layered CVI-processed ceramic matrix has been developed in order to increase the oxidation resistance of continuous fiber-reinforced composites.[1,2] These matrices are aimed at promoting both multiple crack deviation and crack healing so that oxygen ingress is kept as far as possible from the fibrous reinforcement when the composite material is thermomechanically loaded in an aggressive environment. Improving the efficiency of such matrices while avoiding many empirical trial tests has made necessary the setting up of numerical models aimed at predicting some thermochemical and thermomechanical properties of the layered composite materials. In this respect, a first important step consists in obtaining a precise knowledge of the basic properties of each material constitutive of the layered matrix. Previous studies have shown that materials in the Si–B–C system are efficient to get a good oxidation protection in a large temperature range, i.e. from 450 to 1500 °C.[3] Since most of the published works only deal with the improvement of the oxidation resistance of ceramic matrix composites (CMC), no thermomechanical data are available regarding CVI-processed Si–B–C based ceramics, at the exception of silicon carbide. The present study is thus aimed at establishing some thermomechanical properties of various Si–B–C based carbides, i.e. boron carbide B_4C, materials of the Si–B–C system with different boron contents, silicon carbide SiC and boron-doped pyrolytic carbon B_xC_{1-x} further referred to as C(B) in the text.

Since the CVI-processing and the characterization of free standing ceramic materials is always a difficult task, an original method, based on thermomechanical tests performed on matrix-dominated carbon fiber/ceramic matrix microcomposites, has been used to determine the Young's modulus, rupture strength and thermal expansion coefficient of each constituent of the layered matrix as a function of temperature. These properties have been established by an inverse method using a specific testing device previously custom made in our laboratory,[4,5] which allows to determine longitudinal Young's modulus and longitudinal thermal expansion coefficient of coated and uncoated carbon fibers, from room temperature up to 1200 °C, under inert atmosphere.

* Corresponding author. Tel.: +33 5 56 84 47 23; fax: +33 5 56 84 12 25.
E-mail address: camus@lcts.u-bordeaux1.fr (G. Camus).

0955-2219/$ – see front matter © 2007 Elsevier Ltd. All rights reserved.
doi:10.1016/j.jeurceramsoc.2006.12.006

A first simple application regarding the use of these experimental data has then been undertaken through the computation of the thermal residual stresses present from processing in some CMC systems, especially those processed with a layered matrix.

2. Experimental procedure

2.1. Materials

The microcomposites were based on the use of a commercial carbon fiber (XNO_5 from Nippon Graphite Fiber), whose characteristics are well known and reported in Table 1. This fiber has been selected because of its low Young's modulus, its regular and circular cross-section (easily measured by laser diffraction) and its nearly isotropic characteristics. Such characteristics allow (i) to emphasize the part played by the matrix in the global behavior of the microcomposites and (ii) to minimize the calculation uncertainties related to the fiber properties.

The various ceramic matrices were deposited, by chemical vapor infiltration (CVI),[6] on carbon fibers previously mounted on graphite racks. Besides a common CVI-SiC, two different boron carbides, referred to as $B_4C(1)$ and $B_4C(2)$ were obtained through the use of two different processing conditions, resulting in two slightly different chemical compositions (determined using ESCA analysis), see Table 2. Similarly, two materials of the Si–B–C system were also processed, denoted as Si–B–C(1) and Si–B–C(2) in Table 2, where Si–B–C(1) stands for the material with the higher silicon content.

Raman spectroscopy as well as X-ray and TEM analysis have also been performed on all the deposits in order to determine their microstructural organization. Results have shown that, whereas silicon carbide appears to be crystallized (with a faulted β structure), all the other deposits present an amorphous structure. The Raman spectra displayed in Fig. 1 clearly shows that there was neither free silicon nor free aromatic carbon present in the silicon carbide and in the Si–B–C(2) material. Conversely, a limited amount of free carbon was evidenced in the two B_4C and in the Si–B–C(1) material.

Microstructural observations performed by polarized light optical microscopy on the C(B) material allowed to determine the so-called extinction angle, Ae, which is representative of the degree of anisotropy of the material.[7] The measured value of 20° is characteristic of an important anisotropy similar to the one usually observed in the case of a rough laminar pyrocarbon.[8]

Coating thicknesses and related matrix contents of the microcomposites are also reported in Table 2. All the coatings proved to be reasonably regular in thickness along the gauge length of the microcomposites.

Table 1
Characteristics of the pitch-based XNO5 carbon fiber (Nippon Graphite Fiber)

Mean diameter (μm) †	10
Young's modulus (GPa)††	52 (±2)
Stress to failure (MPa) with $L_0 = 50$ mm††	1060 (±175)
Resistivity (Ωm)††	26 (±1) at *RT*
Conductivity (W m^{-1} K^{-1})†	4
Longitudinal thermal expansion coefficient (×10^{-6} °C^{-1})††	0.87 at 22 °C [8.47 × 10$^{-10}T^3$ − 3.33 × 10$^{-6}T^2$ + 4.95 × 10^{-3}T + 7.61 × 10^{-1}] from 22 °C up to 1600 °C (T in °C)
Density††	1.61

† From supplier.
†† After Sauder.[5]

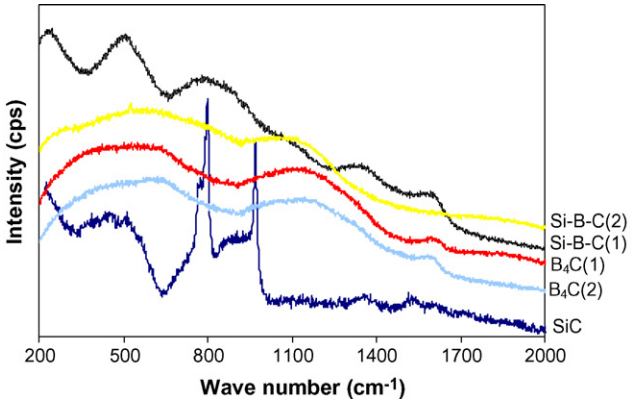

Fig. 1. Raman spectra of the different deposits.

Since high temperature properties were determined up to 1200 °C, i.e. above the processing temperature, samples were systematically heat-treated prior to testing in order to avoid any possible structural change related evolution of the measures. For a standard heat treatment performed at 1200 °C during 30 min under vacuum, both X-rays and Raman analysis did not emphasize any noticeable structural change for the five ceramic materials ($B_4C(1)$, $B_4C(2)$, Si–B–C(1), Si–B–C(2) and SiC). Conversely, in the case of boron-doped carbon, a slight structural reorganization occurred, as evidenced by a decrease of the mean distance between two successive graphitic planes (d_{002}) and a slight increase of the lateral extension of the crystallites (L_C), i.e. two parameters commonly used in the description of carbon structures (Table 3). The orientation parameter Z (intro-

Table 2
Some physical characteristics of the microcomposites

	Si (at.%)	B (at.%)	C (at.%)	Deposit thickness (μm)	Matrix volume ratio (average) (%)
$B_4C(1)$	–	*a*	*b*	2.9 (±0.4)	58
$B_4C(2)$	–	*a* − 4%	*b* + 4%	2.6 (±0.1)	56
Si–B–C(1)	*x*	*y*	*z*	5 (±0.7)	72
Si–B–C(2)	*x* − 31%	*y* + 35%	*z* − 4%	4.5 (±0.7)	71
SiC	50	–	50	6.9 (±0.6)	81
C(B)	–	Few%		6.4 (±0.4)	82

Table 3
Influence of a heat treatment on the structural parameters of the C(B) material determined by X-ray analysis

	d_{002} (Å)	L_c (Å)	Z (°)
C(B)	3.414	30.048	34.56
C(B) heat-treated during 30 min at 1200 °C	3.379	35.601	29.94

duced by Ruland[9] and defined as the width at half the maximum intensity of the distribution function of the graphitic planes) also decreased, meaning therefore that the orientation distribution of these graphitic planes along the deposit axis was less scattered. Results obtained from Raman spectroscopy (Fig. 2) evidenced a narrowing of the peaks subsequently to the heat treatments, which confirms the trend towards a slight structural reorganization.

Remark. It is important of note that, as already mentioned, all these microcomposites were processed in view of emphasizing the behavior of the matrix. Thus, contrary to usual CMC systems for which damage-related non-linearities are promoted along with appreciable strength and moduli, the selected carbon fiber has a low Young's modulus, the fiber content was kept low and no compliant coating was interposed between the fiber and the matrix.

2.2. Thermomechanical testing

Tensile tests were performed from room temperature up to 1200 °C under secondary vacuum (<10^{-3} Pa) on microcomposites with a gauge length of 50 mm, using a specific device described elsewhere[4,5] and schematically drawn in Fig. 3.

Samples were held between two graphite grips using a carbon-based cement (C34 from Ucar). Tests were performed up to rupture at a strain rate of 1% min^{-1}. Strain measurements were derived from grip displacement by using a compliance calibration technique that allows deformation of the load frame to be taken into account. As previously mentioned, in order to avoid possible microstructural changes occuring during the high temperature tests, samples were maintained 30 min prior to testing (i) at the testing temperature in the case of tensile tests and (ii) at 1200 °C in the case of thermal expansion measurements. These last measurements were performed by applying and maintaining constant during sample testing a very low stress onto the microcomposites. The displacement which had to be applied to maintain this imposed stress thus balanced the longitudinal expansion of the sample induced by heating.

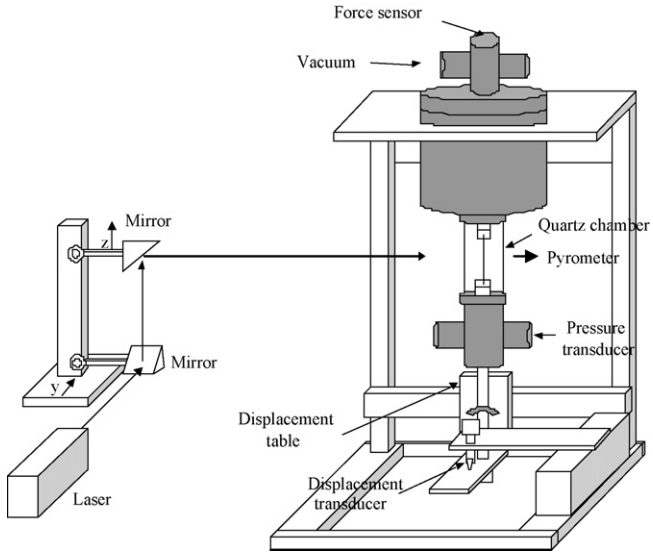

Fig. 3. Schematic diagram of the high temperature fiber testing apparatus.

Specimen heating is obtained by the application of an electric current, which, in the case of a single carbon fiber, leads to a uniform temperature being generated along the specimen.[4] Computations of thermal distributions in the case of a silicon carbide matrix microcomposite, established with a thermal conductivity taken equal to 12 W m^{-1} °C^{-1} for SiC at 1200 °C,[10] have shown that temperature gradient is of about 1 °C between the surface and the heart of the microcomposite whereas its axial component becomes negligible at a distance of less than 1 mm from the cold grip (Fig. 4). Consequently, the C/SiC microcomposite appeared to be mostly uniform in temperature in the radial as well as in the longitudinal direction and, although calculations

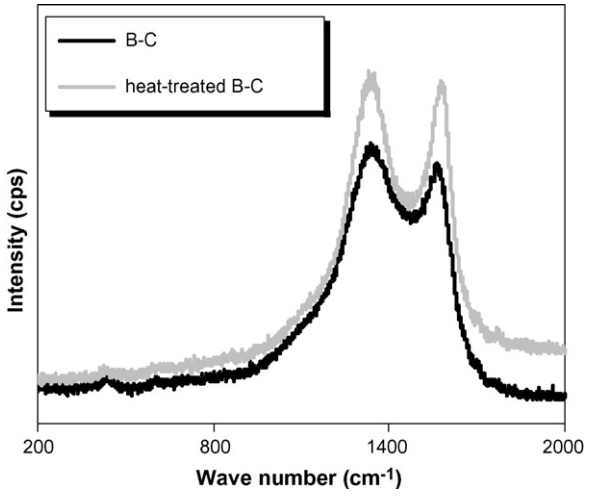

Fig. 2. Influence of a 1200 °C heat treatment on the Raman spectra of C(B).

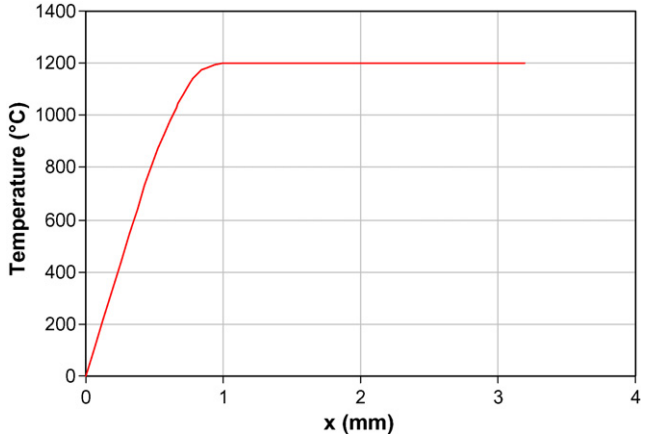

Fig. 4. Calculated axial temperature profile at a microcomposite's end (× represents the distance from the grip).

were not made for the other microcomposites because of a lack of data, it may be inferred that similar results would have been obtained.

Young's modulus and thermal expansion coefficient of the various carbides were derived from the results of the thermomechanical tests performed on microcomposites, using the well-known rule of mixtures as follows:

$$E_c = E_f V_f + E_m V_m \quad \text{which leads to} \quad E_m = \frac{E_c - E_f V_f}{V_m} \tag{1}$$

$$\alpha_c = \frac{E_m V_m \alpha_m + E_f V_f \alpha_f}{E_c} \quad \text{which leads to}$$

$$\alpha_m = \frac{\alpha_c E_c - E_f V_f \alpha_f}{E_m V_m} \tag{2}$$

where E_c is the microcomposite longitudinal Young's modulus, E_f the fiber Young's modulus, V_f the fiber volume ratio, E_m the matrix Young's modulus, V_m the matrix volume ratio and α_c, α_f, α_m are thermal expansion coefficients of the microcomposite, fiber and matrix (respectively).

Calculations, reported in Appendix A, have shown that, in the present case of matrix dominated microcomposites, in terms of volume ratio as well as longitudinal Young's modulus, the rule of mixtures represents an accurate solution of the exact Hashin's two cylinders model.[11] This model is, besides, particularly well suited to the microcomposites used in the present study since it relies on the two basic hypothesis of (i) a perfect bonding between the fiber and the matrix and (ii) two coaxial cylinders with an infinite length. The interfacial bond is likely strong (and therefore close to "perfection") since tensile tests revealed a brittle behavior without any fiber pullout, which is commonly the case with ceramic matrix composites when no compliant interfacial coating and/or reaction product layer is present between the fiber and the matrix.[12]

The well-known Weibull's model[13] was used for the description of the statistical distributions of failure strengths. In this model, failure probability under a uniform stress state is given by:

$$P = 1 - \exp\left[-\left(\frac{V}{V_o}\right)\left(\frac{\sigma}{\sigma_o}\right)^m\right], \tag{3}$$

where m is the shape parameter (often referred to as the Weibull modulus), σ_o the scale factor, V the microcomposite volume under stress, V_o the reference volume (set at $V_o = 1\ \text{mm}^3$ in the present study) and σ is the applied stress.

Probabilities of failure were determined using ranking statistics. Ordering the failure data from smallest to largest and assigning a ranking number i, the probabilities of failure were then assigned by:

$$P_i = \frac{(i - 0.5)}{N}, \tag{4}$$

where N is the total number of specimens.

The statistical parameters were then extracted from strength distributions using the conventional Weibull linear regression estimator.

Rupture stress of brittle materials is sensitive to scale effects. This is related to randomly distributed flaws with varying types and sizes in the material. These effects were described by the following equation, directly derived from Eq. (3).

$$\frac{\sigma'_R(V')}{\sigma_R(V)} = \left(\frac{V}{V'}\right)^{1/m} \tag{5}$$

where V and V' are two different volumes under stress.

3. Results and discussion

3.1. Tensile tests at room temperature

Mechanical characteristics of the different matrices derived from the tests performed in tension at room temperature are summarized in Table 4, in which E_m, σ_{Rm}, ε_{Rm} represent the Young's modulus, the stress to failure and the strain to failure of the matrix, respectively. σ'_{Rm} and ε'_{Rm} refer to normalized failure data, obtained through the use of Eq. (5), for a unique volume V' taken equal to 0.01 mm^3.

Since all the microcomposites behaved in a brittle manner, a noticeable scattering of the failure stresses was always observed. Statistical distributions of strength data were thus determined on batches of about 20 test specimens using the Weibull's model briefly described in the previous section. Obtained results, plotted under a classical Weibull's diagram (Fig. 5), gave access to

Table 4
Mechanical characteristics at room temperature

	C(B)	B_4C(1)	B_4C(2)	Si–B–C(1)	Si–B–C(2)	SiC
Microcomposite's failure stress (MPa)	526 (46)	594 (83)	656 (130)	568 (122)	636 (82)	497 (124)
Average matrix volume V (mm^3)[a]	0.0158	0.0063	0.0049	0.0123	0.0112	0.0194
E_m (GPa)	48 (2)	442 (16)	419 (23)	355 (16)	373 (15)	416 (12)
σ_{Rm} (MPa)	517 (46)	951 (133)	1022 (155)	748 (153)	853 (125)	595 (148)
ε_{Rm} (%)	1.09 (0.09)	0.21 (0.03)	0.25 (0.05)	0.21 (0.04)	0.23 (0.03)	0.14 (0.03)
m	13.4	8.4	7.9	5.5	8.1	4.6
σ_o (MPa)	394	553	553	360	521	278
σ'_{Rm} (MPa)[b]	535	900	933	776	865	687
ε'_{Rm} (%)[b]	1.11	0.20	0.22	0.21	0.23	0.16

Values in parenthesis indicate standard deviation.

[a] Calculated from Table 2.

[b] For a matrix volume $V' = 0.01\ \text{mm}^3$.

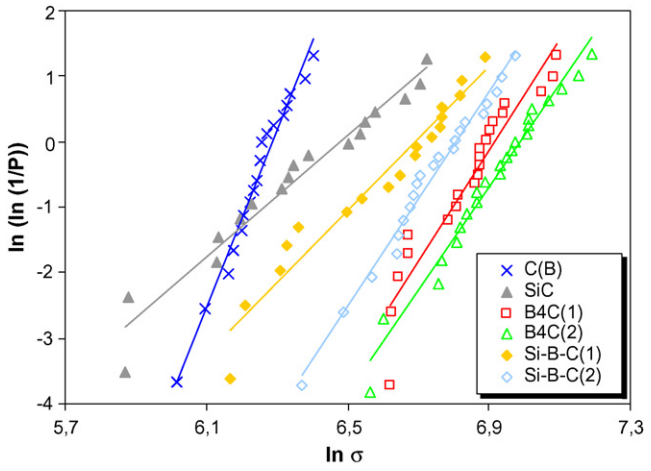

Fig. 5. Weibull diagram for all the deposits.

the Weibull modulus m and to the scale factor σ_o (for the retained reference volume V_o of 1 mm^3).

The Weibull modulus represents the degree of scattering of the fracture data. High values of Weibull modulus are usually related to flaws which are homogeneous in size and well distributed in the material. Conversely, low values are related to flaws which are more scattered in their size and their distribution. It seems therefore that high boron containing materials (B-C, $B_4C(1)$, $B_4C(2)$ and Si–B–C(2)) have less critical flaws than high silicon containing materials (SiC, Si–B–C(1)). Normalized failure data also derived from the tests corroborate these trends.

Not surprisingly, the compliant boron-doped pyrocarbon C(B) material falls apart from this description, i.e. its Weibull modulus has the highest value whereas its failure stress is the lowest. In fact, the lower failure stress is a direct consequence of the low value of the longitudinal Young's modulus, but its remarkably high strain to rupture (i.e. about five times that of the other materials) tends to corroborate the high Weibull modulus: this material, as commonly observed with rough laminar pyrocarbon, is less brittle and flaw sensitive than ceramic materials.[14]

3.2. Tensile tests at high temperature

Fig. 6 shows the evolution of the stress–strain curves of some of the different microcomposites investigated, as a function of temperature. It should be mentioned that, in contrast with the

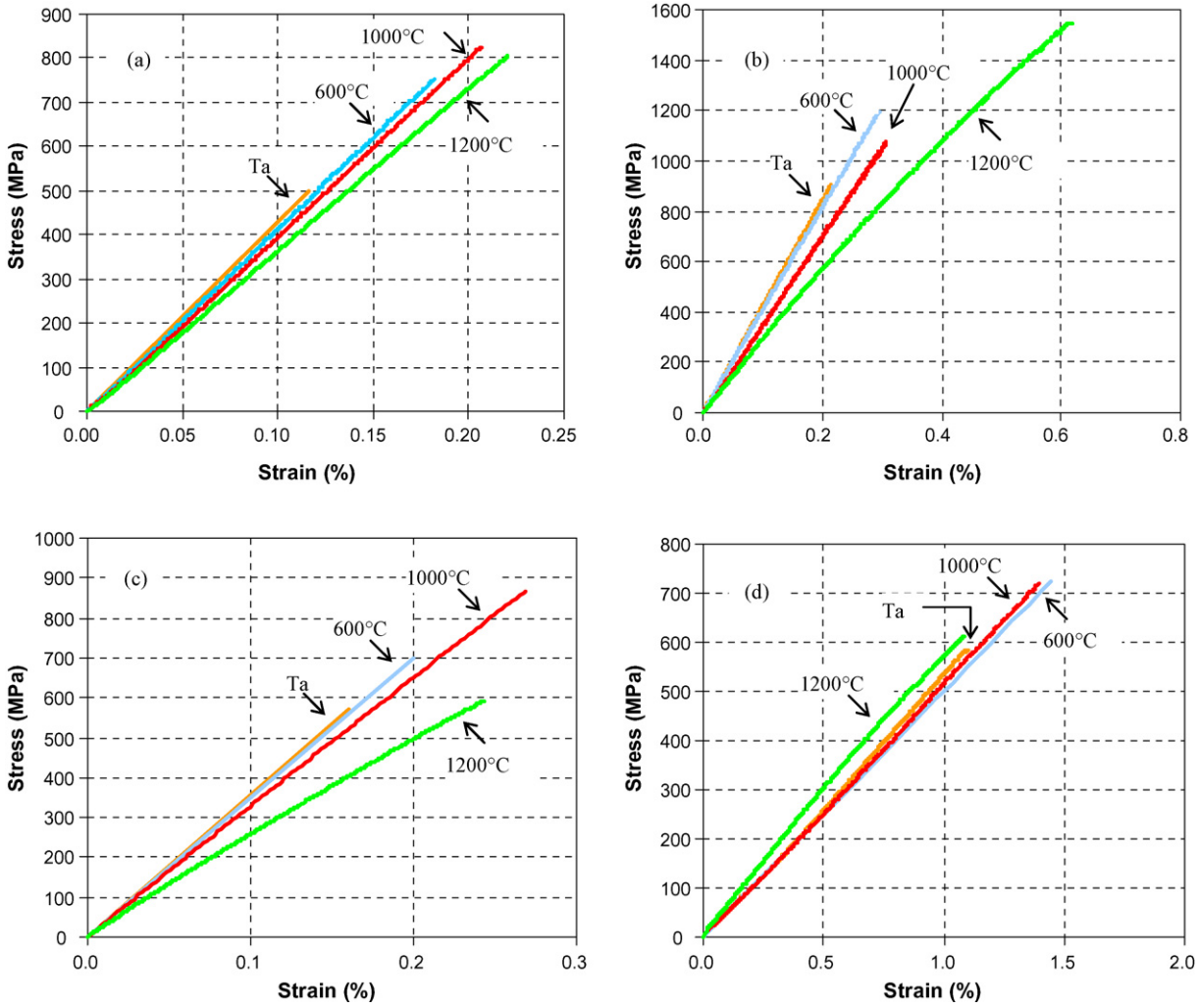

Fig. 6. Evolution of stress–strain curves as a function of temperature for (a) SiC, (b) $B_4C(2)$, (c) Si–B–C(1) and (d) C(B).

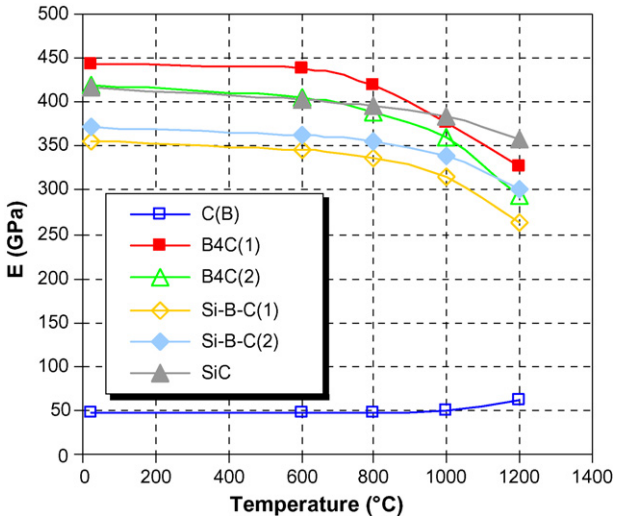

Fig. 7. Young's modulus evolution as a function of temperature.

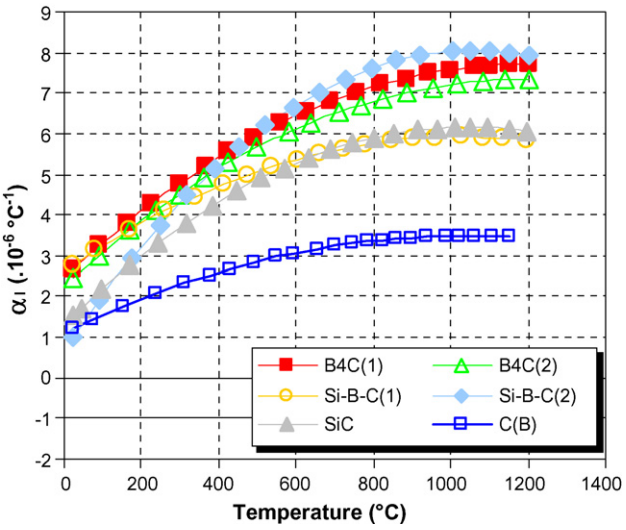

Fig. 8. Evolution of the thermal expansion coefficient as a function of temperature.

previous analysis performed at room temperature, no statistical study has been made regarding high temperature values of the stress to failure. Consequently, no comparison could be made in terms of failure strengths. All the microcomposites exhibit a linear-elastic and brittle behavior from room temperature up to 1000 °C. Over this temperature, i.e. at 1200 °C, and except for the silicon carbide matrix microcomposite, all the other microcomposites exhibit a non-linear behavior. As there is obviously no possibility for multicracking of the matrix (the fiber volume ratio is too low), this non-linearity has to be attributed to a viscoplastic and/or a viscoelastic behavior. Such a time-dependent behavior can then be related to a time-dependent phenomenon present within the fiber, the interface or the matrix. The influence of the fiber should be excluded because (i) the matrix drives the microcomposite behavior and (ii) the C/SiC microcomposite remains linear at 1200 °C. Interface sliding also seems to be excluded because of the likely strong bonding present between the fiber and the matrix. Consequently, it seems that the time-dependent behavior observed at 1200 °C has to be related to the matrix and more precisely to the amorphous boron phases.

Fig. 7 displays, for each constituent, the evolution of the Young's modulus as a function of temperature. For all the deposits but C(B), the Young's modulus decreases in a constant manner with an increase in temperature, which has to be classically related to the progressive weakening of the chemical bonds. Conversely, boron-doped carbon presents a relatively stable modulus up to 800 °C, and then increases continuously at higher temperatures. This increase may be related to a better structural organization and, above all, to a better orientation of the graphitic planes along the deposit axis.

3.3. Thermal expansion coefficients

It may be seen, from Fig. 8, that, for all the studied materials, the thermal expansion coefficients of the various ceramic materials classically increase with temperature. However, it also appears that the CTE values of the boron-rich materials ($B_4C(1)$, $B_4C(2)$, Si–B–C(2)) are systematically higher than these of the silicon-rich materials (Si–B–C(1)), SiC). More investigations need to be performed in order to fully understand this last result.

The CTE values obtained for the boron-doped carbon have been compared with those of different pyrocarbon previously obtained by using the same determination method.[4] The CTE of C(B) thus appeared to be very close to the one of a laminar rough pyrocarbon, which confirms the optical observations performed on the anisotropic texture.

3.4. Thermal residual stresses

As mentioned in Section 1, a first simple application regarding the use of these experimental data is the computation of the thermal residual stresses present from processing in some carbon fiber reinforced ceramic matrix composites. As a matter of fact, residual stresses are usually present in high temperature processed composites (i.e. not only CMC) because of the coefficient of thermal expansion mismatch existing between the reinforcement and the matrix. This is particularly true in the case of carbon fiber reinforced CMC for which this mismatch is quite noticeable. Thus, CVI-processed C/SiC materials, either as 1D model composites[15] or as 2D woven composites,[16] although possessing a thick compliant carbon interphase, always proved to contain matrix microcracks after processing. Conversely, it appears from the works of Lackey et al.[17] and Lamouroux et al.[1] that, when similar ex-PAN carbon fibers were coated with a multilayered matrix $(C/[C/SiC]_n$ and $C/[C(B)/B_4C/C(B)/SiC]_n$ composites, respectively), no cracks were present in the matrix after processing, at least in the case of 1D model composites for the later study.

Computations of thermal residual stresses have been performed on multilayered microcomposites, using the model developed by Warwick and Clyne,[18] which constitutes an improvement of the one previously developed by Mikata and Taya.[19] This model is based on few basic hypothesis, largely similar to those used in the Hashin's two cylinders model, which are: (i) the microcomposite is supposed to be symmetric along its

axis and infinite in length, (ii) interfacial bondings are supposed to be perfect, (iii) the different phases (of finite thickness) are supposed to be isotropic or transversely isotropic (along z-axis) and to behave in a linear elastic manner and (iv) the temperature inside the microcomposite is supposed to be uniform.

Calculations have taken into account experimentally determined evolutions of the thermomechanical characteristics of each constituent as a function of temperature. Regarding the isotropic ceramic materials (i.e. $B_4C(1)$, $B_4C(2)$, Si–B–C(1), Si–B–C(2) and SiC), the temperature-related evolution of their Young's modulus and thermal expansion coefficient was fitted by a polynomial regression of the experimental points (see Figs. 7 and 8). Conversely, since Poisson's ratio were not experimentally measured, their values were all set equal to 0.2, which is an average of the various values found in the literature. Calculations were performed on model microcomposite systems based on an ex-PAN carbon fiber. This kind of fiber and the boron-doped carbon have a markedly transverse isotropic symmetry and, since only the longitudinal thermoelastic coefficients were determined experimentally, the remaining coefficients were also taken from the literature. The choice of the ex-PAN fiber was retained in a view of mimicking the two multilayered-matrix composites previously mentioned. Comparisons have been made with a standard SiC monolayer microcomposite with a C(B) interphase, further referred to as C/C(B)/SiC. All the calculations were performed on microcomposite systems possessing a total thickness of compliant C(B) material and ceramic constituents of 0.4 and 2.8 μm, respectively. The simulated processing temperature was set at 1000 °C, which allows to always remain elastic whatever the material considered.

Of course, the stresses predicted by this simple model based on coaxial cylinders with perfect bonding do not exactly correspond to the stresses present in a real composite since (i) no account is taken of the constraint of the surrounding material and of the interactions with other fibers[20] and (ii) interfacial bonding between each layer are certainly not perfect. Nevertheless, if one considers that (i) some input values were not experimentally measured but only extrapolated and (ii) the requested goal was to clarify some results reported in the literature, it may be inferred that this simple model is largely sufficient to qualitatively interpret results obtained from computations performed on microcomposite systems to real 1D or 2D composites.

Computations of radial and axial residual stresses have shown that, whatever the matrix, (i) the carbon fiber is in radial tension and in axial compression, whereas (ii) the matrix is always in radial tension, which implies a tendency towards debonding at the interface. Figs. 9 and 10 display the calculated residual stresses for a C/C(B)/SiC and a C/[C(B)/SiC]$_4$ microcomposite, respectively. As already mentioned, the multilayered system is directly inspired from the work of Lackey et al.,[17] who studied CVI-processed 2D C/[C/SiC]$_n$ composites and, among other results, observed that no cracks were present in the matrix after processing. It appears from the results displayed in Figs. 9 and 10 that, if the repartition of the compliant C(B) material inside the matrix mainly creates slight stress discontinuities, conversely, the overall tensile stress level of the matrix remains nearly unchanged. Consequently, the reported observation that the multilayered system was undamaged after processing has likely to be related to the fact that a regular repartition of the compliant interphase in the matrix results in thinner ceramics layers. Therefore, if one considers the scale effect already described for brittle materials, higher rupture stress and thus a better resistance to thermal residual stresses should be expected for these thinner layers.

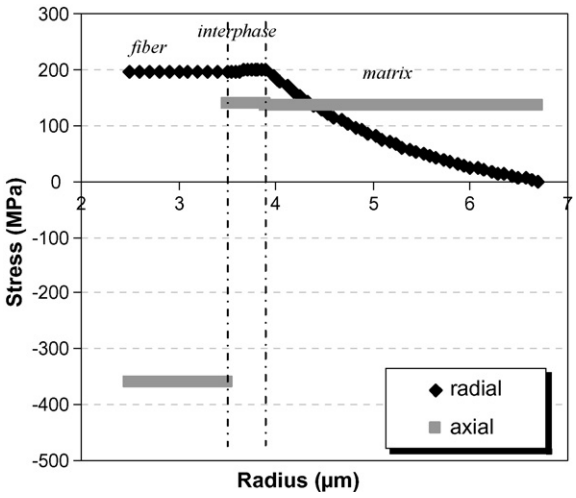

Fig. 9. Calculated residual stress distribution of a C/C(B)/SiC microcomposite cooled from 1000 °C to room temperature.

In order to improve oxidation resistance of carbon-fiber composites, Lamouroux et al.[1,2] developed a multilayered matrix of the type [C(B)/B_4C/C(B)/SiC]$_n$. Results of the computed residual stresses present in a carbon fiber microcomposite with such a matrix are shown in Fig. 11. These results clearly show that, at least for the thicknesses retained in this computation, the B_4C layer and the SiC layer are in a different state of axial tension or compression, which leads to the presence of sudden rises (and drops) in the stress distribution. The mechanical tests that were performed in tension, at room temperature, on composites made with these two multilayered matrices have pointed out different behaviors. Indeed, if no crack deviation

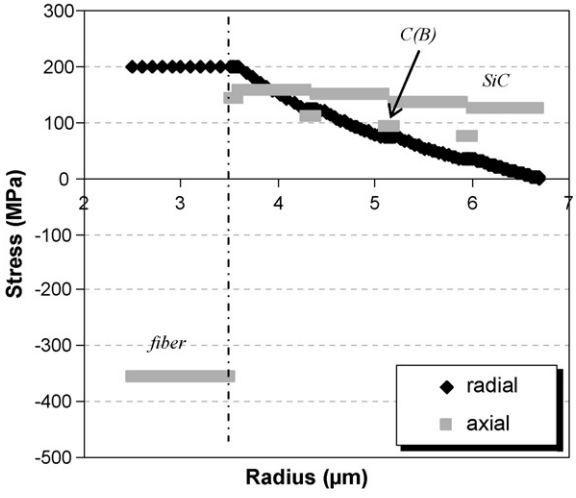

Fig. 10. Calculated residual stress distribution of a C/(C(B)/SiC)$_4$ microcomposite cooled from 1000 °C to room temperature.

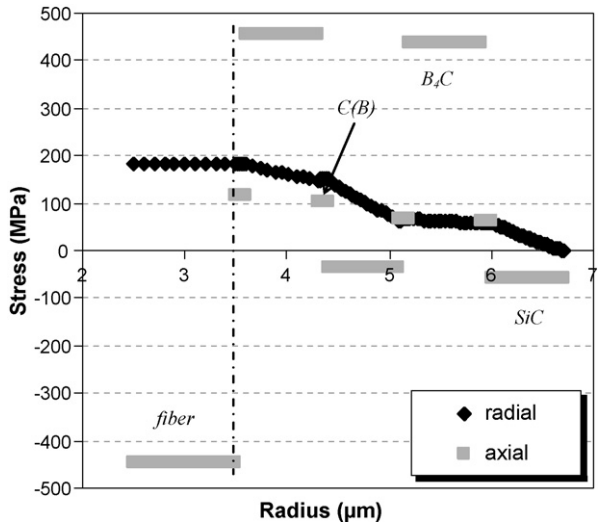

Fig. 11. Calculated residual stress distribution of a C/[C(B)/B_4C/C(B)/SiC]$_2$ microcomposite cooled from 1000 °C to room temperature.

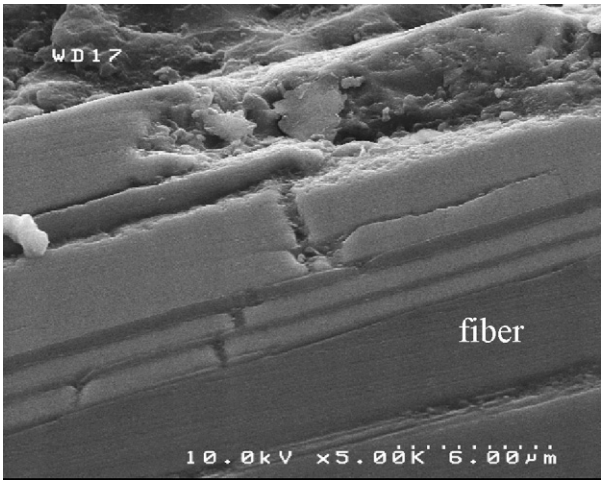

Fig. 12. SEM micrograph showing crack deviation in a C/[C(B)/B_4C/C(B)/SiC]$_n$ minicomposite tensile tested at room temperature.

was explicitly reported by Lackey et al. with their 2D C/[C/SiC]$_n$ composite, such deviations were systematically observed in the case of C/[C(B)/B_4C/C(B)/SiC]$_n$ composites (Fig. 12), either as 2D or 1D model materials.[2,21] It may thus be inferred that the step-like stress distribution created by the alternation of ceramic layers of different nature is likely to favor microcrack deviation between each layer. Of course, care should be taken with this rough interpretation of results since residual stresses and load stresses may have a distinct influence on the thermomechanical properties. Besides, as already discussed, a truly quantitative assessment of the thermal residual stresses present in the aforementioned composite systems would indeed require the use of homogenisation methods and the consideration of imperfect bonding between each layer, which is beyond the scope of this paper. Nevertheless, it is very likely that, at least inside the fiber bundles, computed results should not be fundamentally different from a qualitative point of view.

4. Conclusions

An original method, based on thermomechanical tests performed on CVI-processed carbon fiber/Si–B–C based ceramic matrix microcomposites, has been used to determine the Young's modulus, rupture strength and thermal expansion coefficient of the various ceramic matrices as a function of temperature.

Results have allowed to point out two groups of materials as a function of their chemical composition. Boron-rich materials (B_4C(1), B_4C(2), Si–B–C(2)) have stresses to failure (at room temperature) higher than silicon-rich materials (Si–B–C(1)), SiC) as well as higher thermal expansion coefficients. The analysis of these results led to conclude that this last family of materials likely has critical flaws more scattered in their size and their distribution. Conversely, all the boron-containing materials proved to have a time-dependant mechanical behavior over 1000 °C, which was attributed to the presence of amorphous boron phases.

Finally, the measured thermoelastic values of the ceramic materials have been used to calculate thermal residual stresses in model systems using a layered matrix. These computations have helped to understand some results reported in the literature regarding CVI-processed CMC made of carbon fibers embedded in a layered matrix. Of particular interest was the evidence of an important step-like distribution of the axial residual stresses created by the alternation of ceramic matrix layers of different nature which is believed to have favorably influenced the deviation of matrix cracking inside one of these composite systems.

Acknowledgements

This work was supported by CNRS, Snecma Propulsion Solide and CEA. One of the authors (A.M.) is grateful to CNRS and Snecma Propulsion Solide for support in the form of a research grant. Pr E. Martin (from Bordeaux University) is also gratefully acknowledged for his help in the computation of the thermal residual stresses model.

Appendix A

An accurate and analytical solution establishing the elastic constants of a two concentric cylinders material (i.e. a microcomposite) has been given by Hashin.[10] When the two constituents are both isotropic, this solution reads as follows:

$$\begin{cases} E_L = fE_f + (1-f)E_m + \dfrac{4f(1-f)(\nu_f-\nu_m)^2}{2f((1-2\nu_m)(1+\nu_m))/(E_m) + 2(1+\nu_m)/(E_m) + (1-f)/K_f} \\ \nu_{LT} = f\nu_f + (1-f)\nu_m + \dfrac{f(1-f)(\nu_f-\nu_m)(2((1-2\nu_m)(1+\nu_m))/(E_m) - (1/K_f))}{2f((1-2\nu_m)(1+\nu_m))/(E_m) + 2(1+\nu_m)/(E_m) + (1-f)/K_f} \end{cases} \quad \text{(A1)}$$

where E_L and ν_{LT} are the longitudinal Young's modulus and Poisson's ratio of the microcomposite, whereas K_f stands for the transverse bulk modulus of the fiber which, in case of isotropy, writes:

$$K_f = \frac{E_f}{2(1-2\nu_f)(1+\nu_f)} \quad \text{(A2)}$$

f represents the fiber volume ratio.

The following basic hypothesis were retained:

- the microcomposites were supposed to be infinite in length;
- in any case, the bonding between the fiber and the matrix was supposed to be perfect.

In the present study, the first hypothesis was approximately verified since all the microcomposites sections were always much smaller than their lengths. Besides, the interfacial bond were always likely strong (and therefore close to "perfection") since (i) there was no interphase interposed between the fiber and the matrix and (ii) in any case, tensile tests revealed a brittle behavior without any fiber pullout.

Eq. (A1) constitutes a system of two non-linear equations with two unknown parameters, the Young's modulus E_m and the Poisson's ratio ν_m of the matrix, which can be solved numerically, e.g. with a Newton–Raphson's method (of course once the values of the parameters related to the fiber and the microcomposite have been experimentally obtained).

However, numerous authors emphasize that, in the case of fibers having stiffnesses higher than that of the matrix, the third terms of each equation may be neglected, leading thus to the usual rule of mixtures. This rule of mixtures was directly used in the present work, mainly because the Poisson's ratio of the minicomposites could not be accurately measured (this difficult task remains an open experimental question in the case of small diameter samples). Nevertheless, since the various studied ceramic matrices were all stiffer than the fiber, the relative importance of the third terms had to be subsequently estimated. Calling $C(f)$ the third term of the first of the two equations of the system (A1), one has:

$$E_L(f) = fE_f + (1-f)E_m + C(f) \quad \text{(A3)}$$

with

$$C(f) = \frac{4f(1-f)(\nu_f-\nu_m)^2}{2f((1-2\nu_m)(1+\nu_m))/(E_m) + 2(1+\nu_m)/(E_m) + (1-f)/K_f} \quad \text{(A4)}$$

The relative importance of the neglected term may then be given by the ratio $C(f)/E_L(f)$, which was thus systematically calculated. Fig. 13 displays the evolution of the ratio $C(f)/E_L(f)$ determined as a function of the fiber volume ratio f, in the case of a SiC matrix microcomposite, using the following values:

$\nu_f = 0.3$ $\quad E_f = 52\,\text{GPa}$

$\nu_m = 0.2$ $\quad E_m = 416\,\text{GPa}$ (for SiC)

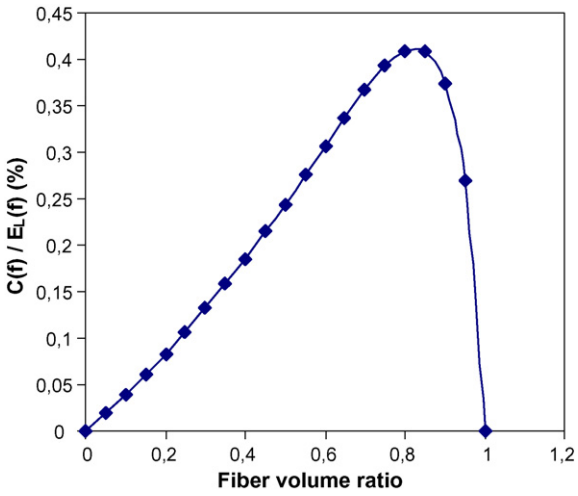

Fig. 13. Evolution of the ratio $C(f)/E_L(f)$ as a function of the fiber volume ratio f in the case of a SiC matrix microcomposite.

It may be seen that, whatever the value taken by f, this ratio remains very small. Consequently, one may conclude that using the rule of mixtures was indeed an accurate approximation.

References

1. Lamouroux, F., Bertrand, S., Pailler, R., Naslain, R. and Cataldi, M., Oxidation-resistant carbon-fiber-reinforced ceramic-matrix composites. *Compos. Sci. Technol.*, 1999, **59**, 1073–1085.
2. Lamouroux, F., Bertrand, S., Pailler, R. and Naslain, R., A multilayer ceramic matrix for oxidation resistant carbon fibers-reinforced CMCs. *Key Eng. Mater.*, 1999, **164–165**, 365–368.
3. Goujard, S., Vandenbulcke, L. and Tawil, H., The oxidation behaviour of two- and three-dimensional C/SiC thermostructural materials protected by chemical-vapour-deposition polylayers coatings. *J. Mater. Sci.*, 1994, **29**, 6212–6220.
4. Sauder, C., Relation microstructure/propriétés à haute température dans les fibres et matrices de carbone. *Thèse de l'Université de Bordeaux I*, 2001.
5. Sauder, C., Lamon, J. and Pailler, R., Thermomechanical properties of carbon fibres at high temperatures (up to 2000 °C). *Compos. Sci. Technol.*, 2002, **62**, 499–504.
6. Naslain, R., Langlais, F. and Fedou, R., The CVI-processing of ceramic matrix composites. *J. Phys. C5*, 1989, **50**, 191–207.
7. Diefendorf, R.J. and Tokarsky, E.W. *Air Force Report AF* 33(615)-70-6-1530, 1971.
8. Dupel, P., Pailler, R. and Bourrat, X., Structure of pyrocarbon infiltrated by pulse-CVI. *Carbon*, 1995, **33**(9), 1193–1204.
9. Ruland, W., X-ray studies on preferred orientation in carbon fibers. *J. Appl. Phys.*, 1967, **38**(9), 3585–3589.
10. Kern, E.L., Hamill, D.W. and Jacobson, K.A., Fabricating SiC parts by chemical vapor deposition. *Adv. Tech. Mater. Investig. Fabric.*, 1968, **14** [II-2B-3].
11. Hashin, Z., Analysis of properties of fiber composites with anisotropic constituents. *ASME J. Appl. Mech.*, 1979, **46**, 543–550.
12. Jouin, J. M., Cotteret, J. and Christin, F., SiC–SiC interphases, Case History. In *Designing Ceramic Interfaces II*, ed. S. D. Peteves. Commission of the European Communities, Petten, 1993, pp. 191–203.
13. Weibull, W., A statistical theory of the strength of materials. *Royal Swedish Institute in Engineering Research*, Report no. 151, 1939.
14. Sauder, C., Lamon, J. and Pailler, R., The tensile properties of carbon matrices at temperatures up to 2200 °C. *Carbon*, 2005, **43**(10), 2054–2065.
15. Lebrun, G.A., Comportement thermomécanique et durée de vie de composites à matrice céramique: théorie et experience. *Thèse de l'Université de Bordeaux 1*, 1996.

16. Camus, G., Guillaumat, L. and Baste, S., Development of damage in a 2D woven C/SiC composite under mechanical loading: I. Mechanical characterization. *Compos. Sci. Technol.*, 1996, **56**, 1363–1372.
17. Lackey, W. J., Vaidyaraman, S. and More, K. L., Laminated C-SiC matrix composites produced by CVI. *J. Am. Ceram. Soc.*, 1997, **80**(1), 113–116.
18. Warwick, C. M. and Clyne, T. W., Development of composite coaxial cylinder stress analysis model and its application to SiC monofilament systems. *J. Mater. Sci.*, 1991, **26**, 3817–3827.
19. Mikata, Y. and Taya, M., Stress field in a coated continuous fiber composite subjected to thermo-mechanical loadings. *J. Compos. Mater.*, 1985, **19**, 554–578.
20. Delannay, F., Thermal stresses and thermal expansion in MMCs. In *Comprehensive Composite Materials, vol. 3 Metal Matrix Composites*, ed. T. W. Clyne. Elsevier, 2000, pp. 341–369.
21. Michaux, A., Amélioration de la durée de vie de composites à matrice céramique à renfort carbone. *Thèse de l'Université de Bordeaux I*, 2003.